



# Photodynamic priming with Vitamin D and ALA-based PDT induces intratumoral immune cell recruitment and signaling pathway activation in cutaneous squamous cell carcinoma

Alan S. Shen<sup>1</sup> · Sanjay Anand<sup>1,2,3</sup> · Cheng-En Cheng<sup>2</sup> · Benjamin Kovacic<sup>4</sup> · Jennifer Powers<sup>4</sup> · C. Marcela Diaz-Montero<sup>4</sup> · Tayyaba Hasan<sup>5</sup> · Edward V. Maytin<sup>1,2,3,6</sup>

Received: 30 December 2025 / Accepted: 20 February 2026  
© The Author(s) 2026

## Abstract

Photodynamic therapy (PDT) is an effective non-invasive treatment for epithelial pre-cancers, yet its efficacy in cutaneous squamous cell carcinoma (SCC) is limited by the immunosuppressive microenvironment of SCC. Vitamin D (VitD) has emerged as a potential neoadjuvant to enhance photodynamic priming in several cancers, but its immunologic effects in SCC remain poorly defined. Here, we investigated how VitD pretreatment modulates local and systemic immune responses to aminolevulinic acid–based PDT in two immunocompetent murine SCC models. VitD combined with PDT significantly amplified hallmarks of immunogenic cell death, including calreticulin and HMGB1 expression. Combination therapy increased intratumoral infiltration of neutrophils, macrophages, dendritic cells, and CD8<sup>+</sup> T cells, while preserving a favorable M1/M2 macrophage ratio and reducing PD-1 expression on cytotoxic T cells. Peripheral immune profiling demonstrated enhanced T-cell activation (CD69) and reduced TIM-3 expression on cytotoxic T cells. Transcriptomic analysis revealed robust enrichment of interferon- $\alpha/\gamma$  signaling and suppression of pro-tumorigenic epithelial–mesenchymal transition and angiogenesis pathways following VitD + PDT. Collectively, these findings demonstrate that VitD reprograms the immune response to PDT in SCC, enhancing cytotoxic immunity while limiting immunosuppressive features. This combination suggests an immune-priming strategy that might be considered, together with immune checkpoint blockade, for SCC and other immunosuppressive cancers.

**Keywords** (4–6) Vitamin D · Photodynamic therapy · Skin cancer · Squamous cell carcinoma · Anti-tumor immunity · Photodynamic priming

---

Alan S. Shen and Sanjay Anand contributed equally.

✉ Edward V. Maytin  
maytine@ccf.org

<sup>1</sup> Cleveland Clinic Lerner College of Medicine, Case Western Reserve University, Cleveland, OH, USA

<sup>2</sup> Department of Biomedical Engineering, Cleveland Clinic Research Institute, Cleveland, OH, USA

<sup>3</sup> Department of Dermatology, Medical Specialty Institute, Cleveland Clinic, Cleveland, OH, USA

<sup>4</sup> Center for Immunotherapy and Precision Immuno-Oncology, Cleveland Clinic, Cleveland, OH, USA

<sup>5</sup> Wellman Center for Photomedicine, Massachusetts General Hospital, Boston, MA, USA

<sup>6</sup> Cleveland Clinic Research, Cleveland Clinic, 9500 Euclid Avenue, Mailstop ND-20, Cleveland, OH 44195, USA

## Introduction

Non-melanoma skin cancers (NMSC), including squamous cell carcinoma (SCC) and basal cell carcinoma (BCC), are the most common of all human malignancies [1–3]. Surgical excision is the first-line treatment for SCC to prevent local invasion and metastases [4–6]. Although locally advanced disease and metastases are relatively uncommon (up to 10% and 1% of cases, respectively), the absolute number of cases is significant and systemic therapy is often required [6]. Immune checkpoint inhibitors (ICIs) have shown promise in advanced NMSC, but only a limited subset of patients respond [4]. Therefore, additional effective therapies and adjuvants for SCC are needed.

Photodynamic therapy (PDT) is a non-invasive, non-scarring, and non-mutagenic treatment for skin cancers and precancers. A precursor drug (5-aminolevulinic acid; ALA)

is preferentially taken up by tumor cells and converted into a photosensitizer, protoporphyrin IX (PpIX). Upon activation with visible light, PpIX generates reactive oxygen species that induce tumor cell death [7]. Direct killing of tumor cells by PDT is well-known, but the concept of *photodynamic priming (PDP)* is relatively new [8, 9]. PDP refers to a collection of PDT-induced mechanisms that occur in surviving but damaged tumor tissue, which together act to enhance the therapeutic response to additional therapies (e.g., chemotherapy or ICIs) [8, 9]. PDP effects include loosening of tumor stroma, induction of immunogenic cytokines, and triggering of immunogenic cell death (ICD). ICD is characterized by expression of damage-associated molecular patterns (DAMPs) that promote recruitment and activation of neutrophils, macrophages, and dendritic cells [10, 11]; these innate immune cells then drive a subsequent, adaptive immune response against the tumor.

To further enhance PDP effects, *Vitamin D (VitD)* has emerged as a promising neoadjuvant due to several complementary actions. First, VitD promotes squamous cell differentiation and increases intracellular PpIX accumulation [12]. Second, VitD can regulate innate and adaptive immunity in the setting of cancer, through VitD receptor-mediated gene expression [13, 14]. Third, a randomized clinical trial in patients with actinic keratoses (AK; squamous pre-cancer) confirmed that high-dose VitD supplementation prior to PDT significantly improves lesion clearance rates [15]. A different clinical trial found that high-dose VitD and PDT can enhance lesion clearance in patients with BCC, particularly for thin BCC tumors [16]. While such preclinical and clinical results highlight the potential utility of VitD + PDT for patients with AK and thin BCC, the question of whether these immune-enhancing mechanisms are operative in fully-developed SCC remained unanswered.

In this study, we used two immunocompetent murine SCC models to characterize the magnitude, time-course, and functional significance of immune changes induced by VitD + PDT compared with each treatment alone.

## Methods

### Cell lines and culture

Murine PDVC57B (PDV) squamous cell carcinoma cells (CancerTools [17]) were originally derived from C57BL/6 keratinocytes via repeated dimethylbenz(a)anthracene (DMBA) treatment [18]. Cells were cultured in Dulbecco's Modified Eagle Medium (DMEM) supplemented with 10% fetal bovine serum and 1% penicillin–streptomycin at 37 °C in 5% CO<sub>2</sub>. Cultures were passaged every 2 days at a 1:3 ratio, and cells at  $\geq 5$  passages were used for in vivo experiments.

### Rationale for SCC tumor models

To evaluate how the anti-tumor immune response to PDT is altered when combined with neoadjuvant VitD, we used two different tumor models. The first model (UV-SCC) was created by exposing mice repeatedly to ultraviolet light, which simulates how humans develop SCC due to chronic sun exposure. The second model (PDV cells, injected subcutaneously in syngeneic C57BL/6 mice) was chosen to help elucidate the immune response after VitD + PDT treatment of well-established, nodular SCC tumors since the response might be different than in the UV-SCC model.

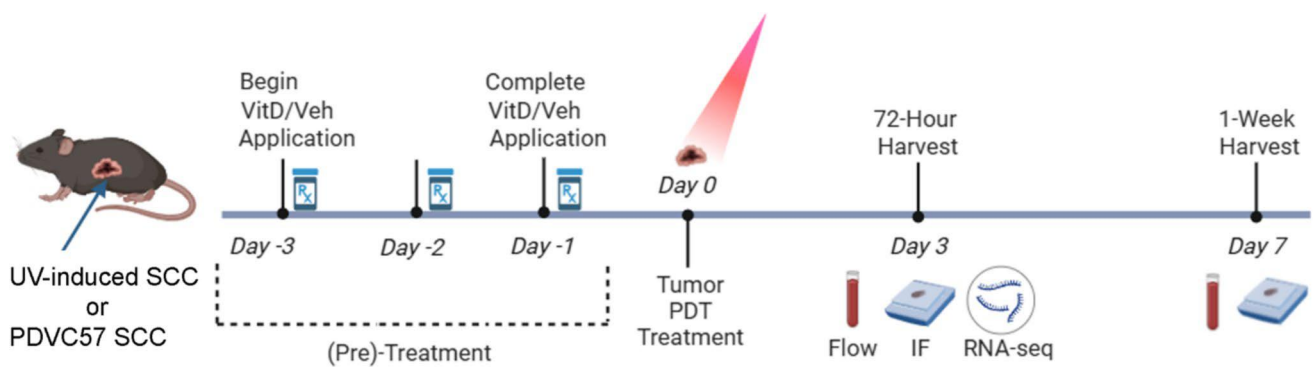


**Fig. 1** Experimental design for VitD pretreatment and PDT in murine SCC models. SCC tumors were generated using either a UV-induced model in SKH-1 hairless mice or a subcutaneous PDVC57B cell-derived model in C57BL/6 mice. VitD pretreatment was administered over 72 h (Days –3 to –1), just prior to PDT on Day 0. Tumors receiving no PDT (VitD alone or vehicle control) were harvested

after the same 72-h pretreatment period. PDT-treated tumors were harvested at 72 h (Day 3) or 1 week (Day 7) post-treatment. Peripheral blood was collected at each tissue harvest for flow cytometry, and tumor tissue was processed for immunofluorescence (both time points) and bulk RNA sequencing (72-h time point only)

Each model was used in time-course experiments as outlined in Fig. 1.

### UV-induced superficial SCC model

Female SKH-1 hairless mice (8 weeks old) were exposed to UV irradiation (80% UVB/20% UVA) three times weekly, beginning at 80 mJ/cm<sup>2</sup> and increasing by 10 mJ/cm<sup>2</sup> weekly to a maximum of 180 mJ/cm<sup>2</sup>. By 20 weeks, mice developed morphologic and histologic features consistent with human SCC. All animal protocols were approved by the Cleveland Clinic IACUC.

### PDVC57 deep SCC model

PDVC57B cells (2–5 × 10<sup>6</sup>) were resuspended in 0.1 mL of a 1:1 Matrigel/DMEM mixture and injected subcutaneously into the left flank of 8-week-old C57BL/6 mice. Tumors reached 5–10 mm in 2–3 weeks.

### Vitamin D pretreatment

For superficial UV-SCC lesions, topical calcitriol ointment (3 µg/g; Vectical) or vehicle (petroleum jelly) was applied daily for 3 days (72 h) prior to PDT [19]. For implanted PDV tumors, calcitriol (1 µg/kg) was administered intraperitoneally once daily for 3 days. An overview of treatment conditions and the samples collected is shown in Fig. 1.

### Photodynamic therapy

UV-SCCs received topical 20% 5-aminolevulinic acid (ALA) in PBS/EDTA/DMSO, followed immediately by blue light exposure (Blu-U; 417 nm, 30 min, 18 J/cm<sup>2</sup>).

PDV tumors received intraperitoneal ALA (200 mg/kg) with a 4-h uptake period, followed by red light illumination (LumaCare xenon source; 633 nm, 100 J/cm<sup>2</sup>). Tumors were shielded with opaque foil templates to confine illumination [11, 19]. Blue light was used for superficial UV-SCCs; red light was selected for PDV tumors due to its deeper penetration of tissues.

### Tissue collection and immunofluorescence

Tumors were excised at 72 h or 1-week post-PDT, fixed in 10% neutral-buffered formalin overnight, and paraffin-embedded. Sections (5 µm) were deparaffinized, rehydrated, and subjected to citrate buffer antigen retrieval. After blocking with 3% normal donkey serum, slides were incubated overnight at 4 °C with primary rabbit antibodies against Ly6G (neutrophils), F4/80 (macrophages), CD86 (M1 macrophages), CD206 (M2 macrophages), CD11c

(dendritic cells), CD3 (T-cells), CD8 (cytotoxic T-cells), FoxP3 (regulatory T-cells), or PD-1 (exhaustion T-cells). All primary antibodies were from Cell Signaling Technology, Danvers, MA. Cy3-conjugated secondary antibodies (Jackson ImmunoResearch Laboratories, West Grove, PA) and DAPI mounting medium (VECTASHIELD) were used for detection. Three high-power fields per tumor were imaged by fluorescence microscopy. Immune cells were counted manually; DAMP expression was quantified by ImageJ [20].

### Peripheral blood flow cytometry

Prior to tumor harvesting, peripheral blood was collected from each mouse via terminal cardiac puncture. Samples were first incubated with Fc block (anti-mouse CD16/CD32, Clone 93) to reduce non-specific antibody binding. Samples were then stained with fluorochrome-conjugated antibodies and analyzed on a BD FACSymphony A5 SORP flow cytometer.

Unless otherwise noted, antibodies for immune profiling were purchased from BD Biosciences and targeted the following: CD45 (Clone 30-F11), Ly6G (1A8), CD11c (HL3), NK1.1 (PK136), CD8 (53–6.7), CD11b (M1/70), CD3e (500A2), CD335/NKp46 (29A1.4), and Ly6C (AL-21). For T regulatory cell identification: CD4 (GK1.5), CD25 (PC61), and CD127 (SB/199). For immune activation and functional classification: CD154 (MR1), CD44 (IM7), CD62L (MEL-14), CD69 (H1.2F3), I-A/I-E (BioLegend; M5/114.15.2), CCR2 (475,301), and CXCR2 (V48–2310). For immune checkpoint markers: PD-1 (J43), PD-L1 (eBioscience; MIH5), ICOS/CD278 (BioLegend; 15F9), and TIM-3 (BioLegend; B8.2C12).

Flow cytometry data were analyzed using FlowJo software (version 10.8; Treestar, Ashland, OR, USA). The gating scheme utilized for each sample has been previously published [19].

### RNA isolation and sequencing

A portion of each tumor (≤ 30 mg) was stored in RNAlater, frozen, and processed (Qiagen RNeasy Mini Kit). RNA concentration and integrity (DV200) were confirmed, and libraries were prepared using Illumina Stranded mRNA Prep with poly(A) selection. Sequencing was performed on an Illumina NovaSeq 6000 (≈ 30 million paired-end reads/sample).

Raw sequencing reads in FASTQ format were aligned to the latest mouse reference genome (GRCm39) using the STAR aligner (version 2.7.11a) [21]. Alignment quality control was conducted using RSeQC, which assesses mapping quality and RNA integrity metrics from the resulting BAM files [22]. Read summarization was carried

out using featureCounts [23], which quantified the number of reads mapped to each gene based on the GENECODE M33 mouse annotation (GRCm39).

Gene-level count data from all samples were merged using an in-house R script. Differential gene expression analysis was performed using the DESeq2 package [24]. DESeq2 normalizes read counts to account for differences in sequencing depth and library composition using the median-of-ratios method. It models gene expression variation using a negative binomial distribution and estimates gene-specific dispersion to account for heteroscedasticity. Statistical significance for differential expression between groups was assessed using the Wald test, and  $p$ -values were adjusted for multiple hypothesis testing using the Benjamini-Hochberg procedure to control the false discovery rate. The final DESeq2 output included a list of differentially expressed genes (DEGs) with associated log<sub>2</sub> fold changes and adjusted  $p$ -values (FDRs).

Gene Set Enrichment Analysis (GSEA) was then performed on the ranked list of DEGs using the clusterProfiler R package [25]. Enrichment was tested against the Hallmark gene sets from the Molecular Signatures Database (MSigDB), which represents 50 curated biological pathways [26]. Visualization of enriched pathways was performed using the dotplot function from the enrichplot R package [27], which displays the enrichment score and adjusted  $p$ -values across all pathways.

## Statistics

A power analysis was performed based on the primary endpoint of neutrophil proportion following either photodynamic therapy (PDT) alone or vitamin D pretreatment plus PDT. Mean and standard deviation estimates were derived from preliminary data on neutrophil responses to PDT in murine actinic keratosis [19]. To detect a 15% difference in group means with 80% power and a significance level of 0.05, a minimum of 4 mice per treatment group was determined to be sufficient.

Data from immunofluorescence cell counts and flow cytometry-derived cellular proportions were analyzed in GraphPad Prism v10.0 (GraphPad Software, San Diego, CA). Group differences were assessed using the nonparametric Kruskal-Wallis test, followed, when significant, by pairwise Mann-Whitney  $U$  tests. These pairwise Mann-Whitney comparisons were prespecified (Veh vs. VitD, Veh vs. VehPDT 72 h, Veh vs. VitD+PDT 72 h, Veh vs. Veh+PDT 1wk, Veh vs. VitD+PDT 1wk, Veh+PDT 72 h vs. VitD+PDT 72 h, Veh+PDT 1 week vs. VitD+PDT 1 week). To control for multiple comparisons testing, raw  $p$ -values from these pairwise comparisons were adjusted using the Benjamini-Hochberg false discovery rate (FDR) procedure. Adjusted  $p$  values were reported using

GraphPad's default significance notation, where  $p < 0.05$  was denoted by one asterisk (\*),  $p < 0.01$  by two asterisks (\*\*),  $p < 0.001$  by three asterisks (\*\*\*), and  $p < 0.0001$  by four asterisks (\*\*\*\*);  $p \geq 0.05$  was considered not significant ("ns"). Data are presented as mean  $\pm$  SEM unless otherwise noted. Significance bars are shown for Veh vs other groups (only the first significant comparison displayed for IF data), as well as for Veh + PDT 72 h vs VitD + PDT 72 h and Veh + PDT 1 wk vs VitD + PDT 1 wk.

For comparisons with  $n = 3$  per group (M1 macrophages, M2 macrophages, PDV IF data), statistical power was insufficient to detect significance reliably; therefore, these results are presented without significance bars and are interpreted as descriptive trends in the data.

## Results

### Vitamin D and PDT-induced changes in expression of damage associated molecular patterns (DAMPs) in UV-SCC tumors

To assess the impact of VitD and PDT on DAMPs, we performed immunofluorescence analysis (IF) of calreticulin and high mobility group box 1 (HMGB1) expression in UV-SCC tumors. Compared with vehicle, VitD, PDT (72 h post-treatment), and VitD + PDT (72 h) each significantly increased calreticulin ( $p < 0.01$ , Fig. 2A) and HMGB1 ( $p < 0.01$ , Fig. 2B). Notably, VitD + PDT at 72 h produced significantly higher levels of both calreticulin and HMGB1 than PDT alone ( $p < 0.01$ ) at the same time point.

### Vitamin D and PDT-induced changes in recruitment of innate immune cells in UV-SCC tumors

Next, to determine how VitD and PDT influence innate immune cell recruitment in UV-SCC tumors, we quantified neutrophils (Ly6G +), dendritic cells (CD11c +), and macrophages (F4/80 +). The number of neutrophils was significantly increased after VitD alone, PDT alone (72 h), and VitD + PDT (72 h), when compared with vehicle (Fig. 3A). VitD + PDT (72 h) also led to significantly higher neutrophil levels than PDT alone (72 h), indicating an additive effect of VitD (Fig. 3A). Similar trends were observed for macrophages (Fig. 3B), and for dendritic cells (Fig. 3C), with effects persisting up to 1-week post-PDT, at least for macrophages.

### Vitamin D and PDT-induced changes in recruitment of adaptive immune cells in UV-SCC tumors

When assessing the effect of VitD and PDT on adaptive immune cell recruitment in UV-SCC tumors, total T cells

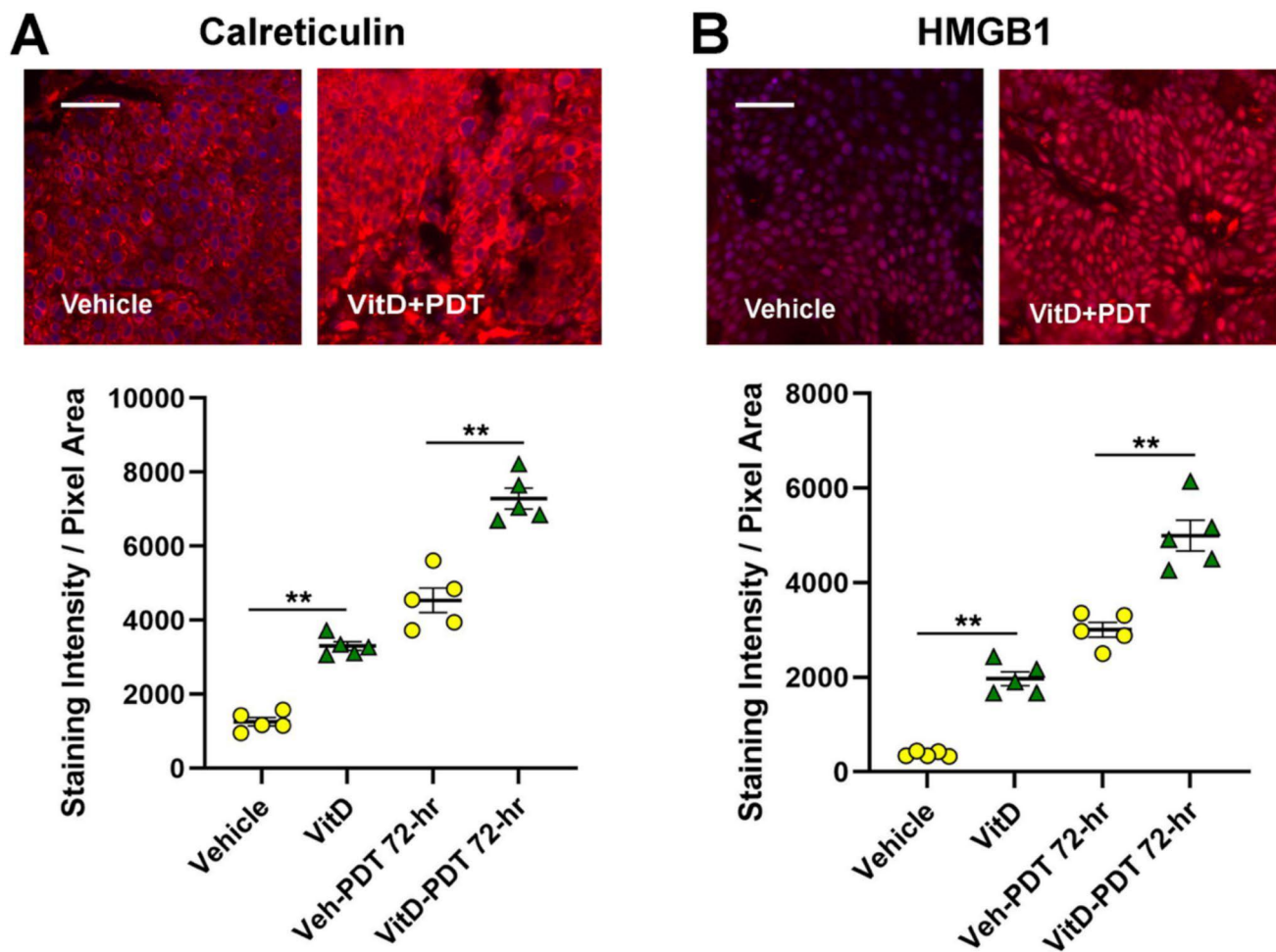


**Fig. 2** Induced expression of the damage-associated molecular pattern (DAMP) proteins *calreticulin* and *HMGB1* in UV-induced SCC lesions following VitD±PDT. For **A** calreticulin and **B** HMGB1, representative immunofluorescent images are displayed above summary graphs that quantify the staining intensity per unit area (pixel) in lesional tissue harvested either before PDT or 72 h after VitD±PDT.  $n=5$  mice per group; each point represents the

average of three fields per lesion from each mouse, with mean  $\pm$  SEM displayed. Statistical analysis used Kruskal–Wallis for overall group comparisons, and when significant, Mann–Whitney U-tests for pairwise comparisons with adjustment for multiple comparisons utilizing the Benjamini–Hochberg correction. Significance levels: (\*\*) $p < 0.01$ . Scale bars = 100  $\mu$ m

(CD3+) were significantly increased after VitD alone, as well as after PDT alone or after VitD + PDT at 72 h and at 1 week post-PDT, relative to vehicle-only controls (Fig. 4A). An additive effect of the VitD + PDT combination was observed at both 72-h and 1 week ( $p < 0.01$ ). A similar pattern was observed for CD8+ T cells (Fig. 4B). T-regs (FoxP3+) were unchanged with VitD alone but increased after PDT and VitD + PDT at 1 week, with higher levels after VitD + PDT than PDT alone (Fig. 4C).

### Vitamin D and PDT-induced changes in immunocytes in the PDVC57B subcutaneous model

To further validate immune cell recruitment patterns in SCC tumors, we examined the second tumor model. In PDVC57B tumors, VitD or PDT alone increased neutrophils, macrophages, and dendritic cells, with greater increases from VitD + PDT (Fig. 5A–C). VitD and PDT each elevated total T cells and CD8+ T cells, further augmented by VitD + PDT (Fig. 5D, E). T-regs increased with PDT and VitD + PDT but not VitD alone (Fig. 5F), which was an observation similar to the UV-SCC model. PD-1+ cells were decreased with VitD, increased with PDT, and returned toward baseline with VitD + PDT (Fig. 5G); this interesting

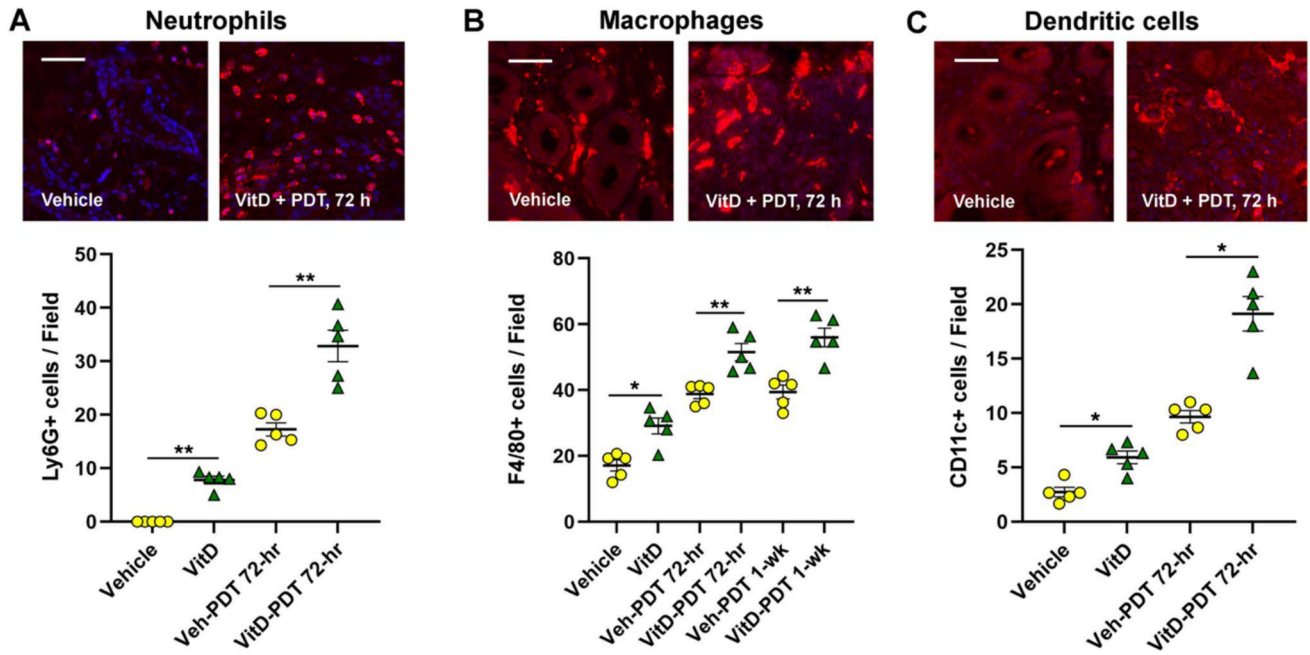


**Fig. 3** Recruitment of innate immune cells: Recruitment of neutrophils, macrophages, and dendritic cells into UV-induced SCC lesions following VitD ± PDT. Representative images of each type of immunostain, and complete quantification of cell numbers per field for: **A** neutrophils; **B** macrophages; and **C** dendritic cells in the SCC tumors at either 72 h or 1 week after no treatment (Vehicle),

VitD only, PDT only, or VitD+PDT are shown, as indicated along the X-axis. Each point represents the average of three fields/lesion (one lesion/mouse); with  $n=5$  mice/group, there are 15 total data points/group, with mean ± SEM displayed. Statistical analysis was performed as in Fig. 2. Significance levels: (\*),  $p < 0.05$ ; (\*\*),  $p < 0.01$ . Scale bars = 100 μm

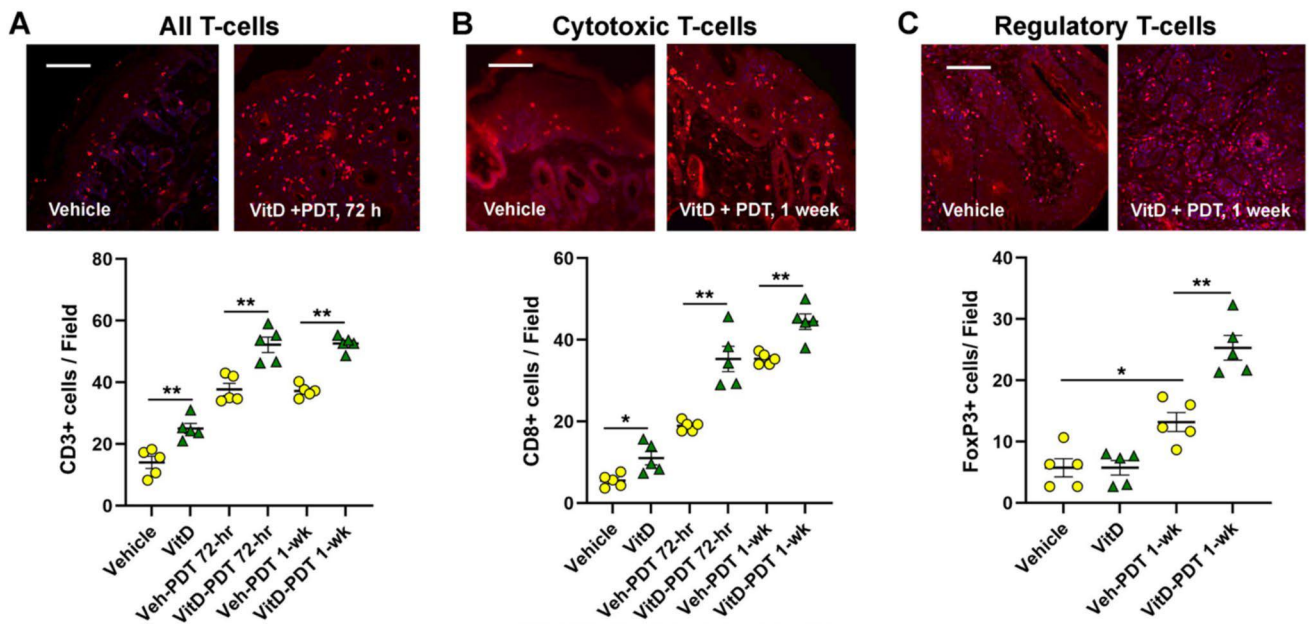


**Fig. 4** Recruitment of adaptive immune cells: T-cells, CD8+ T-cells, and T-regs in UV-induced SCC following VitD ± PDT. Quantification of: **A** total T-cells (CD3+), **B** CD8+ T-cells; and **C** T-regs per field is shown below representative immunofluorescently-stained images of these cells in UV-SCC lesions at 72 h after VitD+PDT. Each point

represents the average of three fields per lesion (one lesion/mouse); with  $n=5$  mice/group, for a total of 15 total data points/group; the mean ± SEM is displayed. Statistical analysis was performed as in Fig. 2. Significance levels: (\*),  $p < 0.05$ ; (\*\*),  $p < 0.01$ . Scale bars = 100 μm

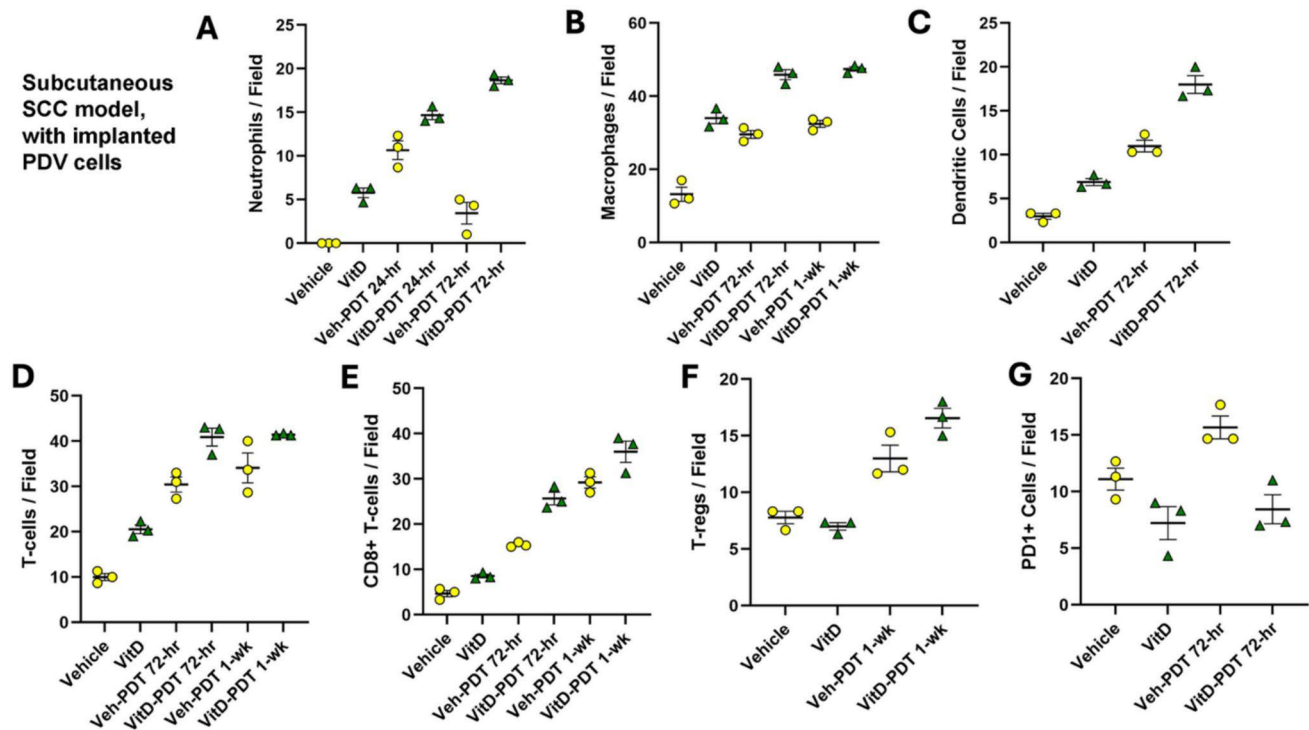


**Fig. 5** Recruitment of innate and adaptive immune cell into implanted PDVCS7B SCC tumors following VitD $\pm$ PDT. Quantification of **A** neutrophils; **B** macrophages; **C** dendritic cells; **D** CD3+ (pan) T-cells; **E** CD8+ T-cells; **F** T-regs; and **G** PDT+ cells per field is shown.  $n=3$  mice per group. Each point represents the

average of three fields per lesion from each mouse, with mean  $\pm$  SEM displayed. While most tumors were harvested at either 72 h or 7 days post-PDT, some samples were harvested at 24 h post-PDT for analysis of early neutrophil recruitment (A)

observation was confirmed later in the UV-SCC model (see below).

### Changes in innate immune cell populations in the peripheral blood after VitD $\pm$ PDT

To compare local tumor immune cell recruitment with data on systemic changes, peripheral blood was collected at the same time as UV-SCC tumor harvest at 72 h post-PDT (see Fig. 1), and analyzed by flow cytometry. Results demonstrated that the proportion of dendritic cells (DCs) amongst total immunocytes (CD45<sup>+</sup> cells) was significantly increased after PDT alone and after VitD + PDT, relative to vehicle ( $p=0.03$  for both, Fig. 6A). DCs also increased after VitD alone and after PDT or VitD + PDT at 1 week, but did not reach statistical significance (Fig. 6A). In contrast, the proportions of neutrophils (Supplemental Fig. 1B) and monocytes (Supplemental Fig. 1C) showed no significant differences across treatment groups.

### Changes in T-cell proportions and activation status in the peripheral blood after VitD $\pm$ PDT

The proportions of total T cells and of CD4<sup>+</sup> or CD8<sup>+</sup> T cells within the T-cell compartment were not significantly altered by treatment (Supplemental Fig. 2A–C). However, T-regs were significantly reduced after PDT or VitD + PDT relative to vehicle alone (at 1 week, but not at 72 h); no change was observed for VitD alone (Fig. 6B). Activated CD69<sup>+</sup> CD4<sup>+</sup> T cells were significantly increased with VitD alone, PDT (72 h, 1 week), or VitD + PDT (72 h, 1 week) as compared with vehicle (Fig. 6C).

Activated CD69<sup>+</sup> CD8<sup>+</sup> T cells were increased significantly, relative to vehicle, after treatment with VitD alone, PDT (72 h, 1 week), and VitD + PDT (72 h, 1 week) (Fig. 6D). At 1 week, the CD69<sup>+</sup> CD8<sup>+</sup> T cells were also significantly increased in VitD + PDT versus PDT alone (Fig. 6D). TIM3<sup>+</sup> CD8<sup>+</sup> T-cells were modestly increased at 72 h and 1-week post-PDT (not significant) compared with vehicle; however, the addition of VitD to PDT significantly reduced TIM3<sup>+</sup> CD8<sup>+</sup> T-cell proportions at both 72-h and 1 week compared with PDT alone (Fig. 6E).

No significant differences were observed in naïve, central memory, effector memory T-cells (Supplemental Fig. 2D–F)

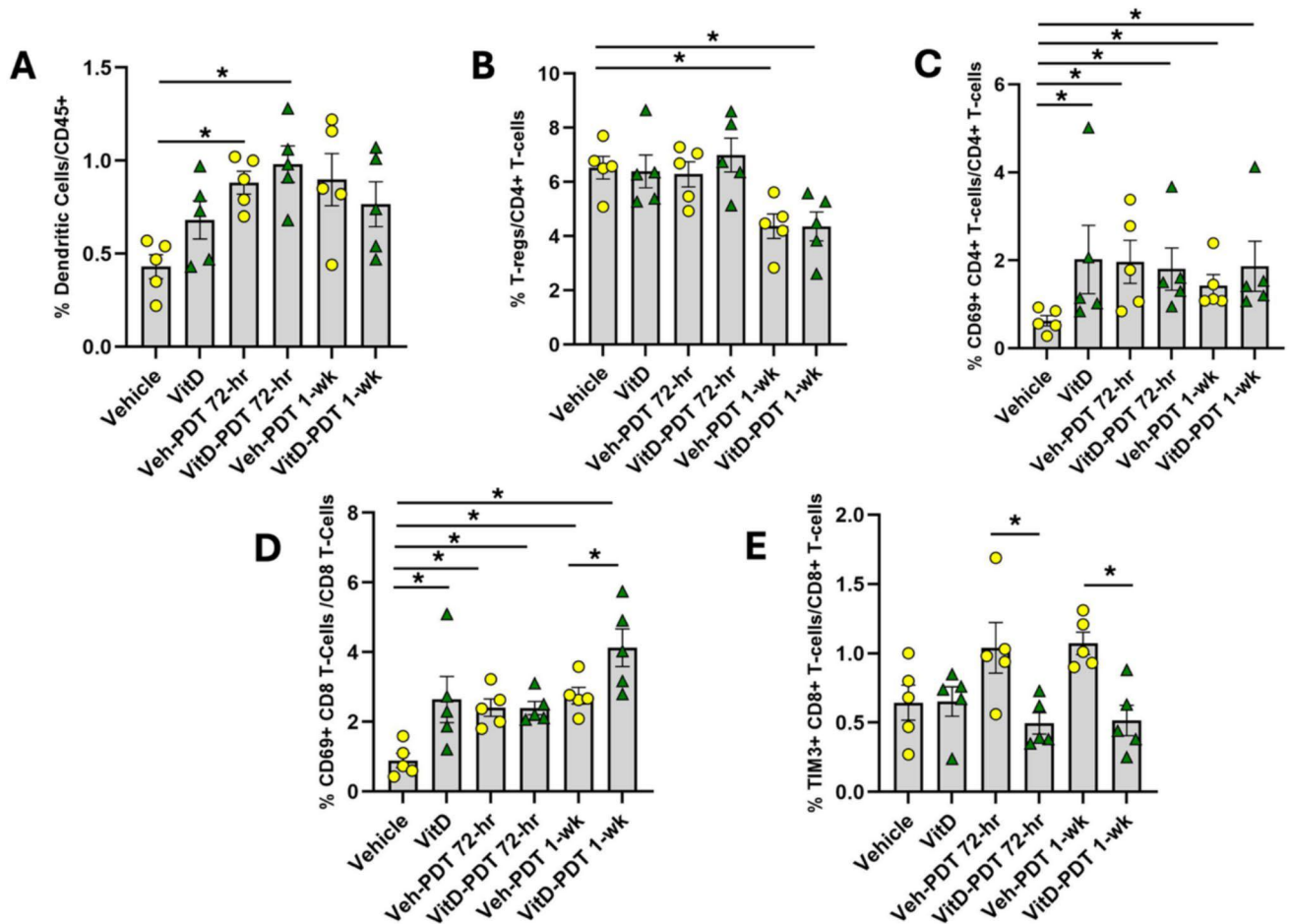


**Fig. 6** Changes in relative numbers of innate and adaptive immunocytes in the peripheral blood of UV-SCC mice. Cell numbers were determined by flow cytometry at 72 h or 1 week after VitD $\pm$ PDT, relative to no-treatment controls. Only those cell types displaying significant changes are presented in this figure; see online Supplement for data from all the cell types that were surveyed. **A** Dendritic cells, as proportion of all

myeloid cells; **B** regulatory T-cells (Tregs; CD25 $^+$ CD127 $^-$ /CD4 $^+$ ); **C** activated helper T cells (CD69+CD4 $^+$ /CD4 $^+$ ); **D** activated cytotoxic T cells (CD69+CD8 $^+$ /CD8 $^+$ ); **E** exhausted cytotoxic T cells (TIM3+CD8 $^+$ /CD8 $^+$ ).  $n=5$  mice per group; points represent individual mice with mean $\pm$ SEM. Statistical analysis was performed as in Fig. 2. (\*), Significance level  $p < 0.05$

or in ICOS $^+$  CD4 $^+$  or ICOS $^+$  CD8 $^+$  T-cells (Supplemental Fig. 2G–H) across treatment groups.

### Transcriptomic analysis reveals pro-tumorigenic signaling pathways affected differentially by vitamin D and PDT

To investigate transcriptional changes induced by treatment, we performed bulk RNA sequencing on UV-SCC tumor tissue after exposure to vehicle, VitD alone, PDT alone, and VitD+PDT groups at 72 h post-treatment. Gene set enrichment analysis (GSEA) results, in which the effects of each treatment relative to vehicle are expressed as a -fold change (Normalized Enrichment Score, NES), are listed in Table 1 along with the statistical significance of each change.

GSEA revealed that PDT and VitD upregulated interferon signaling pathways compared with vehicle. Specifically, PDT significantly increased **interferon- $\alpha$  responses** vs. vehicle (NES = 1.93), as did VitD (NES = 2.02); the combination of VitD+PDT was even more effective at enhancing the interferon- $\alpha$  response (NES = 3.02). A similar pattern was seen for **interferon- $\gamma$  responses**; PDT or VitD enhanced gene activity (NES = 1.63) while the VitD+PDT combination further amplified these effects (NES = 2.75). For both interferon pathways, activity scores for combination VitD+PDT were significantly higher than for PDT alone.

Several other pathways were also significantly upregulated by PDT or VitD, but showed no interaction. *IL2-STAT5 signaling* was enriched by PDT and by VitD, yet the combination of VitD+PDT did not appear to raise the signal any higher than did the individual agents.

**Table 1** Gene set enrichment analysis (GSEA) of signaling pathway activation in murine SCC tumors treated with PDT alone, VD alone, or sequential VD+PDT

Pathway Gene Set (Hallmark)		PDT	VD	VD + PDT	VD + PDT
		vs. Vehicle	vs. Vehicle	vs. Vehicle	vs. PDT
Interferon alpha response	NES	1.93	2.02	3.02	2.14
	<i>p</i> (*)	7.2E-06	1.8E-07	2.5E-09	1.4E-08
Interferon gamma response	NES	1.63	1.83	2.75	1.90
	<i>p</i>	1.6E-04	1.7E-07	2.5E-09	3.4E-04
IL2 – Stat 5 signaling	NES	1.30	1.62	1.49	1.08
	<i>p</i>	0.033	8.6E-05	0.005	0.310
TGF beta signaling	NES	0.87	1.42	-1.10	-1.25
	<i>p</i>	0.793	0.030	0.405	0.190
Epithelial-to-mesenchymal transition (EMT)	NES	1.50	-1.90	-1.40	-1.78
	<i>p</i>	0.003	2.6E-09	0.017	1.1E-06
TNF alpha signaling via NFκ-B	NES	1.08	1.59	1.01	1.04
	<i>p</i>	0.401	2.7E-04	0.560	0.429
Angiogenesis	NES	-1.31	-1.66	-1.57	-1.20
	<i>p</i>	0.177	0.006	0.033	0.256

Murine UV-induced SCC tumors were harvested at 72 h after PDT; after VitD treatment alone (3 days of topical calcitriol); or a 72 h after a combination of VitD pretreatment+PDT. Values shown in the table: NES, normalized enrichment scores (-fold) of pairwise comparisons; *p*, adjusted *P* value (<0.05 is significant). Increases (green) or decreases (red) in pathway activity are indicated. Yellow boxes highlight statistically significant changes

*TGF-β signaling* was modestly enhanced by VitD, but showed no increase with PDT, and showed a trend toward downregulation when VitD and PDT were combined. *TNF-α signaling* was significantly enriched only by VitD, but not by VitD + PDT.

Conversely, two pathways were specifically downregulated in the presence of VitD. *Epithelial–mesenchymal transition (EMT)* was slightly increased after PDT (NES = 1.50), but decreased after VitD treatment (NES = -1.90), and was also decreased after combination VitD + PDT, suggesting that VitD has a dominant effect in suppressing EMT. *Angiogenesis* pathway genes were also significantly suppressed by VitD, alone and together with PDT. PDT alone also suppressed angiogenesis, but the trend was not statistically significant.

### Vitamin D induces changes in the tumor microenvironment that favor anti-tumor immune stimulation

The large numerical increases in innate and adaptive immune cells recruited locally after VitD treatment seems likely to increase overall anti-tumoral immune functions,

but further evidence is needed. In that regard, two changes in specific immune cell subtypes are indicators of likely improvement in functional outcome. First, the ratio of proinflammatory (M1) to quiescent (M2) macrophages was observed to change in the presence of VitD. Each type of macrophage (M1 CD86 + macrophages, Fig. 7A; and M2 CD206 + macrophages, Fig. 7B) was increased after VitD, PDT, or VitD + PDT, but to different degrees. As a result, the ratio of M1/M2 was reduced by PDT alone, yet maintained after VitD or VitD + PDT (Fig. 7C). Thus, M1-mediated anti-tumor activity seems to be suppressed by PDT, but VitD prevents that undesirable side effect.

Second, we observed that PD1 + (exhausted) T cell numbers were reduced in the presence of VitD relative to vehicle (Fig. 7D). When examining specific T-cell subsets by double labeling, both the PD1 + CD3 + T-cells (Fig. 7E) and the cytotoxic PD1+CD8+ T-cells (Fig. 7F) were significantly reduced by the VitD + PDT combination.

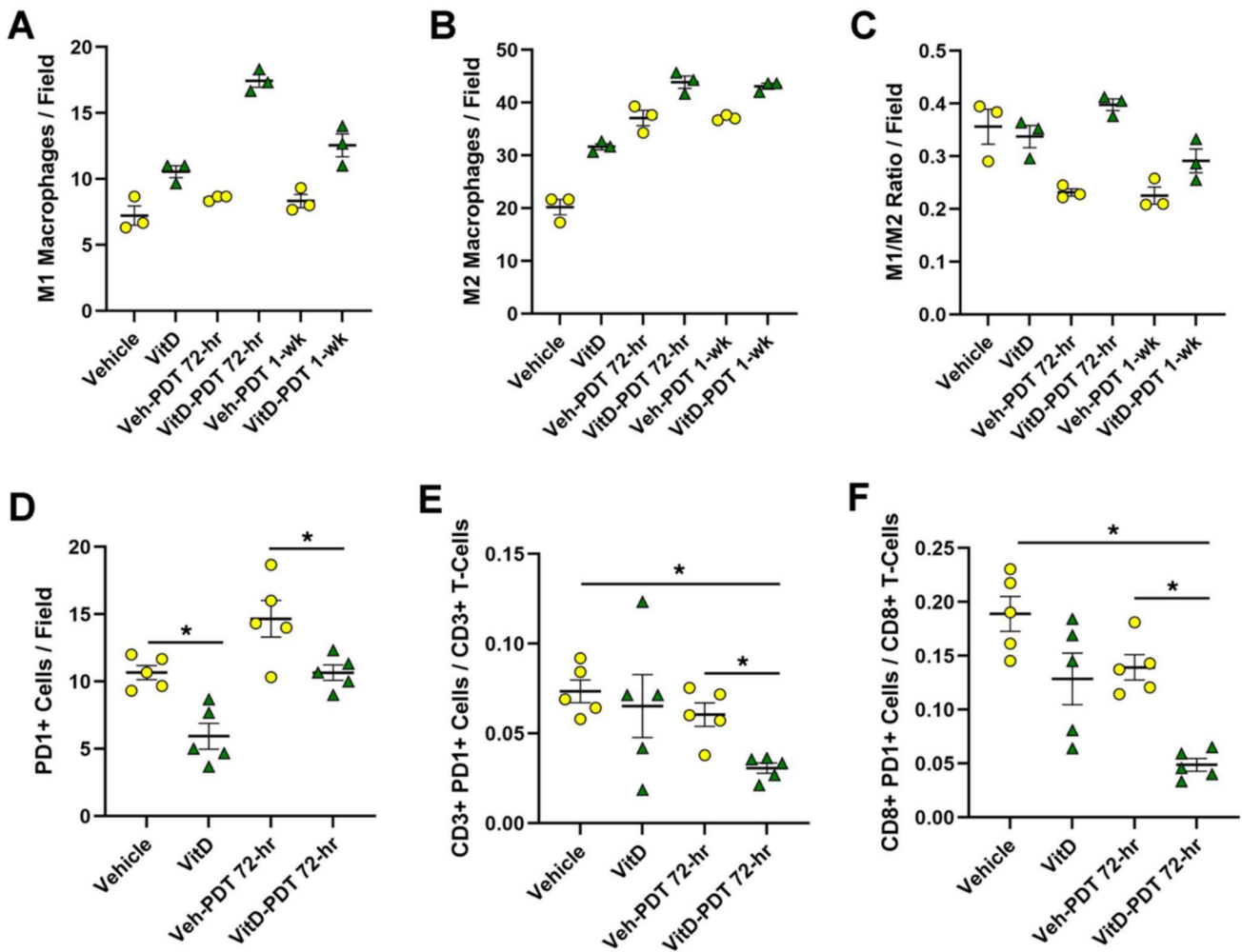


**Fig. 7** Vitamin D pretreatment induces changes in macrophages and in PD1-expressing T cells that are likely to improve overall anti-tumor immune action after PDT. Tissue sections from UV-SCC tumors were harvested at 72 h after VitD±PDT, and immunostained cells counted and quantified as shown in the graphs. *Macrophage subsets*: **A** M1 macrophages, CD86+; **B**, M2 macrophages, CD206+; **C** M1/M2 macrophage ratio,  $n=3$  mice per group; each

point represents the average of three fields per lesion from each mouse, with mean±SEM displayed. *PD1-expressing T-cell subsets*: **D** PD1+ cells **E** CD3+PD1+ T-cells **F** and CD8+PD1+ T-cells. For **D–F**, there were  $n=5$  mice (lesions) per group, three fields per lesion averaged from each mouse, with mean±SEM displayed. (\*), statistical analysis using Kruskal–Wallis tests and Mann–Whitney *U*-tests for pairwise comparisons,  $p < 0.05$

## Discussion

This study was motivated by a desire to better understand the phenomenon of *photodynamic priming* (PDP) in squamous cell carcinoma (SCC) treated with photodynamic therapy (PDT), either in the absence or presence of VitD as a neoadjuvant. PDP is a series of events that occur after partial damage to a tumor, leading to triggering of innate and adaptive anti-tumor immune responses [8–11]. In the case of Vitamin D, prior work in several systems has demonstrated a strong pro-therapeutic effect involving immune upregulation when VitD is used as a pretreatment prior to PDT (reviewed in [12]). In the current study, we show that neoadjuvant VitD and PDT markedly reshapes the tumor immune

landscape in cutaneous SCC. Changes observed in SCC in mice after VitD + PDT involve components of both the innate and adaptive immune systems, and these changes are typically larger in magnitude after VitD + PDT than after either treatment alone.

*Innate immune responses* to damage induced by VitD and PDT in SCC tumors involve immunogenic cell death (ICD) and recruitment of various myeloid cells. For example, robust upregulation of DAMPs (calreticulin and HMGB1) was observed simultaneously with a local increase in neutrophils, macrophages, and dendritic cells. All of these effects occurred after PDT or VitD alone, but were much stronger after combined VitD + PDT. Given the role of DAMPs in activating APCs [28] and priming adaptive

immunity, these findings suggest that VitD amplifies the earliest immune-activating events initiated by PDT. Interestingly, PDT and VitD appeared to have selective and opposing effect upon macrophage subtypes. After PDT alone, M2 macrophages were selectively increased (two-fold), whereas M1 macrophages barely changed (~ 1.2-fold) (Fig. 7A–C), representing a shift toward an immunosuppressive phenotype. However, adding VitD to the PDT regimen elevated M1 macrophages at the expense of M2, boosting the M1/M2 ratio and creating a more favorable environment for anti-tumor activity (Fig. 7A–C). VitD appears to induce a qualitative reprogramming of macrophages that counters PDT-induced M2 expansion by greatly increasing M1 cells, thereby prolonging the anti-tumor immune response.

Important changes within the *adaptive immune compartment* were also observed. For example, we saw robust recruitment of CD3 + CD8 + (cytotoxic) T cells into tumors, although the functional benefits of this may be counteracted by increased FoxP3<sup>+</sup> T-regs after PDT or VitD + PDT (Fig. 4). VitD reduced PD-1<sup>+</sup> T-cells relative to vehicle controls (Fig. 5G), and VitD + PDT further reduced PD-1 expression relative to PDT alone (Fig. 5G, Fig. 7D–F), suggesting that VitD may counteract checkpoint upregulation after PDT. The latter observation is consistent with prior research in non-small cell lung cancer (NSCLC) [29], where VitD was shown to decrease checkpoint marker expression on cytotoxic T cells.

While the changes in relative numbers of the various immune cell subtypes recruited to SCC tumors after VitD and/or PDT were indisputable, we sought additional evidence that these cellular changes might have functional consequences. For this question, transcriptomic analysis (Table 1) provides at least some functional context for the histologically observed changes in immune cell subsets. GSEA revealed strong enrichment of interferon (IFN)- $\alpha$  responses (potentially linked to antigen presentation and innate immune activation [30]) and of IFN- $\gamma$  responses (associated with cytotoxic T-cell effector function [30]) after PDT, VitD, and VitD + PDT. These changes align with findings of increased innate and adaptive immune cell infiltration, suggesting that recruited cells were not only more abundant but also functionally primed. TNF- $\alpha$  signaling (consistent with pro-inflammatory cytokine release and neutrophil recruitment [31]) was upregulated by VitD, in line with increases in intratumoral myeloid cells, while IL2–STAT5 signaling (critical for T-cell proliferation and survival [32]) was moderately enriched. VitD (alone or together with PDT) suppressed pro-tumorigenic EMT and angiogenesis pathways, suggesting additional pathways for limiting tumor progression.

Immune profiling of peripheral blood offered findings that supplement the tumor histological and transcriptional

data. Circulating dendritic cells were increased by PDT and combination treatment, suggesting that enhanced systemic antigen presentation might occur in parallel with the increase in tumor-infiltrating dendritic cells. Peripheral T-regs were reduced by VitD + PDT despite being increased intratumorally, suggesting recruitment from circulation rather than systemic expansion. While this trafficking could represent a local counter-regulatory response to PDT-induced inflammation, the observed rise in circulating activated CD69<sup>+</sup> T cells and decline in TIM3<sup>+</sup> exhausted CD8<sup>+</sup> T cells in the VitD + PDT group indicate that overall effector quality is improved, not blunted. While no major differences were observed across naïve, central memory, effector memory, and ICOS<sup>+</sup> T-cell subsets, this may reflect the limited one-week observation period. Finally, although PD-1 was included in the flow cytometry panel, minimal PD-1 expression was observed in peripheral blood. This finding is consistent with prior literature demonstrating that PD-1 expression is predominantly localized to tumor-infiltrating lymphocytes rather than peripheral blood T cells [33].

Our data help to refine the current body of knowledge about how VitD affects immunity in the context of treating cancer with PDT. VitD can be immunosuppressive in chronic inflammatory conditions where it downregulates pro-inflammatory cytokines [34–36], reinforces tolerance, and inhibits development of autoimmune diseases [34, 37, 38], but VitD can also be immunostimulatory during infections by enhancing innate antimicrobial responses via cathelicidins, defensins, and PRR activation [39]. In regards to battling cancer, many of the known roles of VitD and VDR-dependent gene transcriptional activity appear helpful, with a list of actions that includes: (1) suppression of tumor proliferation, angiogenesis, and tumor survival [40, 41]; (2) shifting of the local microenvironment toward an effector-dominant state [40, 42]; (3) increasing NK and CD8<sup>+</sup> T cell activity in glioblastoma and breast cancer [43, 44]; (4) enhancing Th1 cytokine production and reducing immune checkpoint activity in NSCLC [29]; (5) increasing CD8<sup>+</sup> T cell density in colorectal cancer [45]; and (6) improving survival via strengthened immune signatures in melanoma [46]. Although we had known previously that VitD enhances PpIX photosensitizer accumulation in tumors [47], and alters cytokine secretion by cancer-associated fibroblasts [48], our current study has delineated several previously unrecognized anti-tumor immune activities of VitD in SCC, either when administered alone or together with PDT.

This study has some limitations. First, neutrophils and monocytes in our FACS studies were defined only by surface markers, preventing their distinction from myeloid derived suppressor cells (PMN-MDSCs or M-MDSCs). However, the transcriptomic data indicate a predominantly pro-inflammatory state with reduced angiogenesis; since MDSCs

typically promote immunosuppression and angiogenesis, the immune cells observed here are unlikely to represent suppressor subsets. Second, our UV-SCC model (chosen to mimic field cancerization and human SCC development) can be quite variable in terms of tumor size and morphology. To partially address this, a more-uniform SCC model (PDV) was studied in parallel and found to engender similar immune effects as the UV-SCC tumors. Third, our RNA-seq analyses were limited to 72 h post-PDT, a timepoint that captures innate and early adaptive responses but may miss later changes. Finally, we were unable to quantify CD4<sup>+</sup> T cells by immunofluorescence due to technical challenges. In future studies we hope to address the above limitations and conduct functional experiments to ask whether VitD + PDT can synergize with immune checkpoint blockade to improve tumor resolution. Future experiments will also address whether anti-EMT and anti-angiogenesis activities (suggested by our transcriptomic data) can lower rates of metastases after VitD + PDT in a murine tumor model. Ultimately, the VitD + PDT combination should be investigated in human clinical trials of SCC for its potential to improve therapeutic outcomes and serve as an immune-priming strategy.

In summary, data in this report collectively show that VitD enhances PDT immune effects by amplifying the magnitude of immune activation and qualitatively reprogramming it. The combination treatment promotes IFN-driven cytotoxic responses, increases M1 macrophages, reduces inhibitory checkpoints (PD-1, TIM3), suppresses EMT and angiogenesis, and shifts the immune landscape toward more effective cell-mediated immunity.

**Supplementary Information** The online version contains supplementary material available at <https://doi.org/10.1007/s00262-026-04347-6>.

**Author contributions** Alan Shen, Sanjay Anand, Marcela Diaz, Tayyaba Hasan, and Edward Maytin contributed to the study conception and design. Material preparation, data collection and analysis were performed by Sanjay Anand, Cheng-En Cheng, Alan Shen, Benjamin Kovacic, and Jennifer Powers. The first draft of the manuscript was written by Alan S. Shen and all authors commented on previous versions of the manuscript. All authors read and approved the final manuscript.

**Funding** Research reported in this publication was supported by the National Cancer Institute of the National Institutes of Health under Award Number 5P01CA084203. NIH provided approximately 80% of total project costs (~\$200,000) with the remaining 20% covered by institutional funds. The content is solely the responsibility of the authors and does not necessarily represent the official views of the National Institutes of Health.

**Data availability** All data supporting the findings of this study are available within the paper and its Supplementary Information.

## Declarations

**Conflict of interest** The authors have no relevant financial or nonfinancial interests to disclose.

**Open Access** This article is licensed under a Creative Commons Attribution-NonCommercial-NoDerivatives 4.0 International License, which permits any non-commercial use, sharing, distribution and reproduction in any medium or format, as long as you give appropriate credit to the original author(s) and the source, provide a link to the Creative Commons licence, and indicate if you modified the licensed material. You do not have permission under this licence to share adapted material derived from this article or parts of it. The images or other third party material in this article are included in the article's Creative Commons licence, unless indicated otherwise in a credit line to the material. If material is not included in the article's Creative Commons licence and your intended use is not permitted by statutory regulation or exceeds the permitted use, you will need to obtain permission directly from the copyright holder. To view a copy of this licence, visit <http://creativecommons.org/licenses/by-nc-nd/4.0/>.

## References

1. Global Burden of Disease Cancer Collaboration (2019) Global, regional, and national cancer incidence, mortality, years of life lost, years lived with disability, and disability-adjusted life-years for 29 cancer groups, 1990 to 2017: a systematic analysis for the global burden of disease study. *JAMA Oncol* 5:1749–1768. <https://doi.org/10.1001/jamaoncol.2019.2996>
2. Donaldson MR, Coldiron BM (2011) No end in sight: the skin cancer epidemic continues. *Semin Cutan Med Surg* 30:3–5. <https://doi.org/10.1016/j.sder.2011.01.002>
3. Rogers HW, Weinstock MA, Feldman SR, Coldiron BM (2015) Incidence estimate of non-melanoma skin cancer (keratinocyte carcinomas) in the US population, 2012. *JAMA Dermatol* 151:1081–1086. <https://doi.org/10.1001/jamadermatol.2015.1187>
4. Tanese K, Nakamura Y, Hirai I, Funakoshi T (2019) Updates on the systemic treatment of advanced non-melanoma skin cancer. *Front Med (Lausanne)* 6:160. <https://doi.org/10.3389/fmed.2019.00160>
5. Neidecker MV, Davis-Ajami ML, Balkrishnan R, Feldman SR (2009) Pharmacoeconomic considerations in treating actinic keratosis. *Pharmacoeconomics* 27:451–464. <https://doi.org/10.2165/00019053-200927060-00002>
6. Ascierto PA, Schadendorf D (2022) Update in the treatment of non-melanoma skin cancers: the use of PD-1 inhibitors in basal cell carcinoma and cutaneous squamous-cell carcinoma. *J Immunother Cancer* 10:e005082. <https://doi.org/10.1136/jitc-2022-005082>
7. Correia JH, Rodrigues JA, Pimenta S et al (2021) Photodynamic therapy review: principles, photosensitizers, applications, and future directions. *Pharmaceutics* 13:1332. <https://doi.org/10.3390/pharmaceutics13091332>
8. De Silva P, Saad MA, Thomsen HC et al (2020) Photodynamic therapy, priming and optical imaging: potential co-conspirators in treatment design and optimization—a Thomas Dougherty Award for Excellence in PDT paper. *J Porphyrins Phthalocyanines* 24:1320–1360. <https://doi.org/10.1142/s1088424620300098>
9. Obaid G, Celli JP, Broekgaarden M et al (2024) Engineering photodynamics for treatment, priming and imaging. *Nat Rev Bioeng* 2:752–769. <https://doi.org/10.1038/s44222-024-00196-z>
10. Ortenzio MP, Anand S, Travers JB et al (2025) Immunomodulatory effects of photodynamic therapy for skin

- cancer: potential strategies to improve treatment efficacy and tolerability. *Photochem Photobiol* 00:1–15. <https://doi.org/10.1111/php.70008>
11. Anand S, Govande M, Yasinchak A et al (2021) Painless photodynamic therapy triggers innate and adaptive immune responses in a murine model of UV-induced squamous skin pre-cancer. *Photochem Photobiol* 97:607–617. <https://doi.org/10.1111/php.13350>
  12. Anand S, Hasan T, Maytin EV (2024) Treatment of nonmelanoma skin cancer with pro-differentiation agents and photodynamic therapy: preclinical and clinical studies (review). *Photochem Photobiol* 100:1541–1560. <https://doi.org/10.1111/php.13914>
  13. Wei R, Christakos S (2015) mechanisms underlying the regulation of innate and adaptive immunity by vitamin D. *Nutrients* 7:8251–8260. <https://doi.org/10.3390/nu7105392>
  14. Hutchinson PE, Pringle JH (2022) Consideration of possible effects of vitamin D on established cancer, with reference to malignant melanoma. *Pigment Cell Melanoma Res* 35:408–424. <https://doi.org/10.1111/pcmr.13040>
  15. Bullock TA, Negrey J, Hu B et al (2022) Significant improvement of facial actinic keratoses after blue light photodynamic therapy with oral vitamin D pretreatment: an interventional cohort-controlled trial. *J Am Acad Dermatol* 87:80–86. <https://doi.org/10.1016/j.jaad.2022.02.067>
  16. Maytin EV, Zeitouni NC, Updyke A et al (2025) High-dose oral vitamin D in combination with photodynamic therapy can accelerate the clearance rate of basal cell carcinoma: a randomized clinical trial. *Photodiagnosis Photodyn Ther* 55:104704. <https://doi.org/10.1016/j.pdpdt.2025.104704>
  17. PDVC57B Cell Line. In: *CancerTools.org*. <https://cancertools.org/cell-lines/pdvc57b-151630/>. Accessed 13 Aug 2025
  18. Quintanilla M, Haddow S, Jones D et al (1991) Comparison of ras activation during epidermal carcinogenesis in vitro and in vivo. *Carcinogenesis* 12:1875–1881. <https://doi.org/10.1093/carcin/12.10.1875>
  19. Anand S, Shen A, Cheng C-E et al (2024) Combination of vitamin D and photodynamic therapy enhances immune responses in murine models of squamous cell skin cancer. *Photodiagnosis Photodyn Ther* 45:103983. <https://doi.org/10.1016/j.pdpdt.2024.103983>
  20. NIH Image to ImageJ: 25 years of image analysis | *Nature Methods*. <https://www.nature.com/articles/nmeth.2089>. Accessed 13 Aug 2025
  21. Mapping RNA-seq Reads with STAR - Dobin - 2015 - Current Protocols in Bioinformatics - Wiley Online Library. <https://currentprotocols.onlinelibrary.wiley.com/doi/https://doi.org/10.1002/0471250953.bi1114s51>. Accessed 13 Aug 2025
  22. Wang L, Wang S, Li W (2012) RSeQC: quality control of RNA-seq experiments. *Bioinformatics* 28:2184–2185. <https://doi.org/10.1093/bioinformatics/bts356>
  23. Liao Y, Smyth GK, Shi W (2014) FeatureCounts: an efficient general purpose program for assigning sequence reads to genomic features. *Bioinformatics* 30:923–930. <https://doi.org/10.1093/bioinformatics/btt656>
  24. Love MI, Huber W, Anders S (2014) Moderated estimation of fold change and dispersion for RNA-seq data with DESeq2. *Genome Biol* 15:550. <https://doi.org/10.1186/s13059-014-0550-8>
  25. Wu T, Hu E, Xu S et al (2021) ClusterProfiler 4.0: a universal enrichment tool for interpreting omics data. *Innovation* 2:100141. <https://doi.org/10.1016/j.xinn.2021.100141>
  26. Liberzon A, Birger C, Thorvaldsdóttir H et al (2015) The molecular signatures database (MSigDB) hallmark gene set collection. *Cell Syst* 1:417–425. <https://doi.org/10.1016/j.cels.2015.12.004>
  27. Yu G (2025). Enrichplot: visualization of functional enrichment result. R package, version 1.30.4. <https://https://doi.org/10.18129/B9.bioc.enrichplot>
  28. Jentho E, Weis S (2021) DAMPs and innate immune training. *Front Immunol* 12:699563. <https://doi.org/10.3389/fimmu.2021.699563>
  29. Li P, Zhu X, Cao G et al (2022) 1 $\alpha$ , 25 (OH) 2D3 reverses exhaustion and enhances antitumor immunity of human cytotoxic T cells. *J Immunother Cancer* 10:e003477. <https://doi.org/10.1136/jitc-2021-003477>
  30. Zhang X, Wang S, Zhu Y et al (2021) Double-edged effects of interferons on the regulation of cancer-immunity cycle. *Oncoimmunology* 10:1929005. <https://doi.org/10.1080/2162402X.2021.1929005>
  31. Parameswaran N, Patial S (2010) Tumor necrosis factor- $\alpha$  signaling in macrophages. *Crit Rev Eukaryot Gene Expr* 20:87–103. <https://doi.org/10.1615/critrevueukargeneexpr.v20.i2.10>
  32. Moriggl R, Topham DJ, Teglund S et al (1999) Stat5 is required for IL-2-induced cell cycle progression of peripheral T cells. *Immunity* 10:249–259. [https://doi.org/10.1016/S1074-7613\(00\)80025-4](https://doi.org/10.1016/S1074-7613(00)80025-4)
  33. Piersiala K, da Farrajota Neves Silva P, Hjalmarsson E et al (2021) CD4+ and CD8+ T cells in sentinel nodes exhibit distinct pattern of PD-1, CD69, and HLA-DR expression compared to tumor tissue in oral squamous cell carcinoma. *Cancer Sci* 112:1048–1059. <https://doi.org/10.1111/cas.14816>
  34. Yin K, Agrawal DK (2014) Vitamin D and inflammatory diseases. *J Inflamm Res* 7:69–87. <https://doi.org/10.2147/JIR.S63898>
  35. Aranow C (2011) Vitamin D and the immune system. *J Investig Med* 59:881–886
  36. Fenercioglu AK (2024) The anti-inflammatory roles of vitamin D for improving human health. *Curr Issues Mol Biol* 46:13514–13525. <https://doi.org/10.3390/cimb46120807>
  37. Krajewska M, Witkowska-Sędek E, Rumińska M et al (2022) Vitamin D effects on selected anti-inflammatory and pro-inflammatory markers of obesity-related chronic inflammation. *Front Endocrinol*. <https://doi.org/10.3389/fendo.2022.920340>
  38. Shen AS, Johnson JS, Kerns ML (2023) Dietary factors and hidradenitis suppurativa. *Dermatol Ther (Heidelb)* 13:3007–3017. <https://doi.org/10.1007/s13555-023-01056-1>
  39. Bishop E, Ismailova A, Dimeloe S et al (2021) Vitamin D and immune regulation: antibacterial, antiviral, anti-inflammatory. *JBMR Plus* 5:e10405. <https://doi.org/10.1002/jbmr.10405>
  40. Feldman D, Krishnan AV, Swami S et al (2014) The role of vitamin D in reducing cancer risk and progression. *Nat Rev Cancer* 14:342–357. <https://doi.org/10.1038/nrc3691>
  41. El-Sharkawy A, Malki A (2020) Vitamin D signaling in inflammation and cancer: molecular mechanisms and therapeutic implications. *Molecules* 25:3219. <https://doi.org/10.3390/molecules25143219>
  42. Jeon S-M, Shin E-A (2018) Exploring vitamin D metabolism and function in cancer. *Exp Mol Med* 50:1–14. <https://doi.org/10.1038/s12276-018-0038-9>
  43. Kim H, Kim J, Sa JK et al (2022) Calcipotriol, a synthetic vitamin D analog, promotes antitumor immunity via CD4+T-dependent CTL/NK cell activation. *Biomed Pharmacother* 154:113553. <https://doi.org/10.1016/j.biopha.2022.113553>
  44. Karkeni E, Morin SO, Bou Tayeh B et al (2019) Vitamin D controls tumor growth and CD8+ T cell infiltration in breast cancer. *Front Immunol* 10:1307. <https://doi.org/10.3389/fimmu.2019.01307>
  45. Dias Costa A, Kim S, Zhang J et al (2023) Impact of vitamin D on the colon tumor immune microenvironment: results of a randomized clinical trial of preoperative vitamin D supplementation in patients with stage I-III colon cancer. *JCO*

- 41:3607–3607. [https://doi.org/10.1200/JCO.2023.41.16\\_suppl.3607](https://doi.org/10.1200/JCO.2023.41.16_suppl.3607)
46. Muralidhar S, Filia A, Nsengimana J et al (2019) Vitamin D-VDR signaling inhibits Wnt/ $\beta$ -catenin-mediated melanoma progression and promotes antitumor immunity. *Cancer Res* 79:5986–5998. <https://doi.org/10.1158/0008-5472.CAN-18-3927>
47. Anand S, Wilson C, Hasan T, Maytin EV (2011) Vitamin D3 enhances the apoptotic response of epithelial tumors to aminolevulinate-based photodynamic therapy. *Cancer Res* 71:6040–6050. <https://doi.org/10.1158/0008-5472.CAN-11-0805>
48. Anbil S, Pigula M, Huang H-C et al (2020) Vitamin D receptor activation and photodynamic priming enables durable low-dose chemotherapy. *Mol Cancer Ther* 19:1308–1319. <https://doi.org/10.1158/1535-7163.MCT-19-0791>

**Publisher's Note** Springer Nature remains neutral with regard to jurisdictional claims in published maps and institutional affiliations.